Molecular Basis for Environment Sensing by a Nucleoid-Structuring Bacterial Protein Filament

Xiaochuan Zhao[1#], Jacob M. Remington[1#], Severin T. Schneebeli[1], Stefan T. Arold[2,3], Jianing Li[1*]

1 Departments of Chemistry and Materials Science, University of Vermont, Burlington VT 05405
2 King Abdullah University of Science and Technology (KAUST), Computational Bioscience Research Center (CBRC), Biological and Environmental Science and Engineering (BESE), Thuwal, 23955-6900, Saudi Arabia
3 Centre de Biologie Structurale, CNRS, INSERM, Université de Montpellier, 34090 Montpellier, France

*Email: jianing.li@uvm.edu
# These authors contributed equally.

Abstract:
The histone-like nucleoid structuring (H-NS) protein controls the expression of hundreds of genes in Gram-positive bacteria through its capability to coat and condense DNA. This mechanism requires the formation of superhelical H-NS protein filaments that are sensitive to temperature and salinity, allowing H-NS to act as an environment sensor. We use multiscale modeling and simulations to obtain detailed insights into the mechanism of H-NS filament's sensitivity to environmental changes. Through the simulations of the superhelical H-NS filament, we reveal how different environments induce heterogeneity of H-NS monomers. Further, we observe that transient self-association within the H-NS filament creates temperature-inducible strain and might mildly oppose DNA binding. At last, we probe different H-NS–DNA complex architectures and show that complexation enhances the stability of both, DNA and H-NS superhelices. Overall, our results provide unprecedented molecular insights into the environmental sensing and DNA interactions of a prototypical nucleoid-structuring bacterial protein filament.

Keywords: H-NS protein, DNA binding, multiscale modeling, protein polymer, stability, mechanical property.

Despite the lack of an envelope-enclosed nucleus, a bacterial cell can organize its dynamic nucleoid with the nucleoid-associated proteins (NAPs) in a hierarchical fashion.[1-3] Many bacterial NAPs contribute to both the organization of the nucleoid and the control of gene expression. The 137-residue H-NS protein[4-7] abundant in gram-negative bacteria is among the 18 different NAPs whose three-dimensional (3D) structures were characterized. It has been investigated as a model system by us[8-10] and others[11-25]. These studies showed that H-NS dimers can assemble into a superhelical structure and preferentially recognizes AT-rich DNA strands. On the atomistic level, and for reasons of feasibility, these studies concentrated on self-associations between H-NS domains and H-NS dimers,[13, 16, 19, 26-33] or on the association between an H-NS domain and DNA.[18, 25, 34-40] It remains elusive on the molecular level how a full-length H-NS filament[8] interacts with the DNA strand and how this complex system responds to different environmental signals. Herein, we endeavored to fill this knowledge gap via extensive molecular dynamics (MD) simulations of H-NS filaments in absence and presence of DNA.

H-NS possesses three functional domains (Figure 1): An N-terminal dimerization domain (site1), a central dimerization domain (site2) and a C-terminal DNA-binding domain (DNAbd).[41] DNAbd is attached to site2 *via* a flexible linker that contributes to DNA and autoinhibitory interactions.

Site1 and site2 are connected through a helix, and mediate H-NS polymerization through site1–site1 and site2–site2 associations.[42] Whereas site1 dimerization is constitutive, site2 dimerization is sensitive to environmental changes.[9, 33] Increases in temperature and/or salinity destabilize site2 dimerization and hence H-NS filament formation, releasing the coated DNA for gene expression. This environment sensing mechanism helps pathogenic bacteria optimize their behavior when inside warm-blood hosts, but can also be adapted to suit bacteria within other habitats.[10] Despite the lack of full-length or DNA-bound H-NS structures, nuclear magnetic resonance (NMR) studies suggest that the DNAbd can move freely in the H-NS polymer, but attaches to site1 in the monomer.[9] An earlier simulation study[43] identified three possible binding modes between the DNAbd site of H-NS and a short AT-rich DNA strand. The most stable mode likely involves a full insertion of the $Q^{112}G^{113}R^{114}$ motif into the DNA minor groove, which is consistent with prior solution NMR observations.[41] More recently, the DNA binding modes of H-NS and similar proteins were suggested to be switched by the addition of counter ions.[24, 44] Building on prior knowledge, we modeled the superhelical H-NS filament with full-length monomers in this work, to provide a comprehensive view of H-NS domain interactions, filament stability, environment sensing, and DNA binding. Such details are fundamental to understand bacterial growth[45, 46] and adaptive evolution,[10, 47, 48] and may inspire strategies to combat bacterial multidrug resistance.[49]

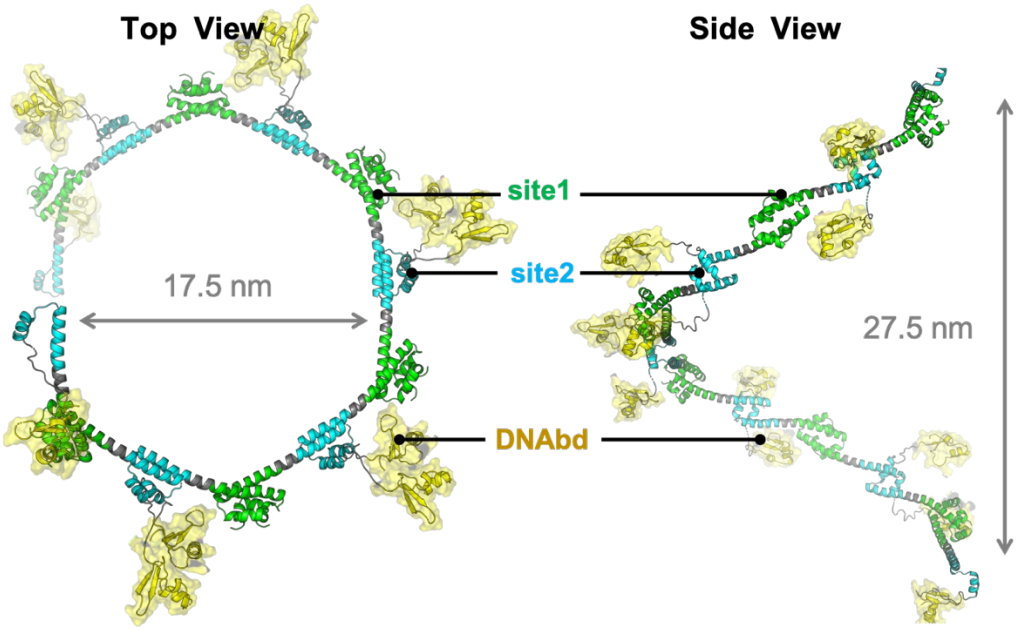

Figure 1. Illustration of our filament model comprised of 12 H-NS monomers (26,067 atoms). In the cartoon, green, cyan, and yellow indicate the site1 (residues 1–44), site2 (resides 52–82), and DNAbd (residues 93–137) domains. The diameter (d=17.5 nm) and pitch (p=27.5 nm) of the right-handed helical model (PDB templates: 3NR7 and 2L93) are labeled. Due to the flexible linker region, DNAbd can adopt multiple positions relative to site1 and site2 in the absence of DNA. In the sequence, the coloring of letters is consistent with the cartoon, with the linker regions annotated in black. The $Q^{112}G^{113}R^{114}$ motif key for DNA binding is highlighted with a yellow background.

Using the full-length H-NS sequence of *Salmonella typhimurium* (UniprotID: P0A1S2) and the superhelical filament architecture (PDB 3NR7), we first constructed the filament model of 12 full-length monomers for a complete helical turn with periodic boundary conditions in the Z-axis (see SI). Given that the local root-mean-square deviation (RMSD) of H-NS monomers were stable after 60 ns in a 200-ns simulation (Figure S1), we performed 100-ns all-atom (AA) simulations under three different conditions, and a 1.3-μs coarse-grained (CG) simulation at a resolution of 6 CG sites/monomer (parameterized with H-NS dimers under the same condition, see SI). To examine the structural stability, we defined the global RMSD of the filament using a CG representation (each CG site at the centers-of-mass of residue 2-82), with the perfect superhelix as a reference. Averaged in the last 20 ns of two AA simulation replicas, the global RMSD of the H-NS filament was 2.7 ± 0.9 nm under our standard condition (0.15 M NaCl, 293 K). Our CG simulation (global RMSD = 2.4 ± 0.4 nm) confirmed this level of fluctuation on a microsecond timescale. Further, our AA simulations showed that the global RMSD of the H-NS filament was increased to 3.3 ± 1.3 nm under high salinity (0.50 M NaCl, 293 K) and to 4.7 ± 1.3 nm under a high temperature condition (0.15 M NaCl, 313 K), indicating higher levels of deformation of the filament. Nevertheless, the helical pitch remained largely unchanged along the Z-dimension, only fluctuating within a narrow range between 27.4 and 27.6 nm under all three conditions. However, there was a 13-16% drop in the filament circumference projected on the XY-plane under a high salt or temperature condition (Figure 2B).

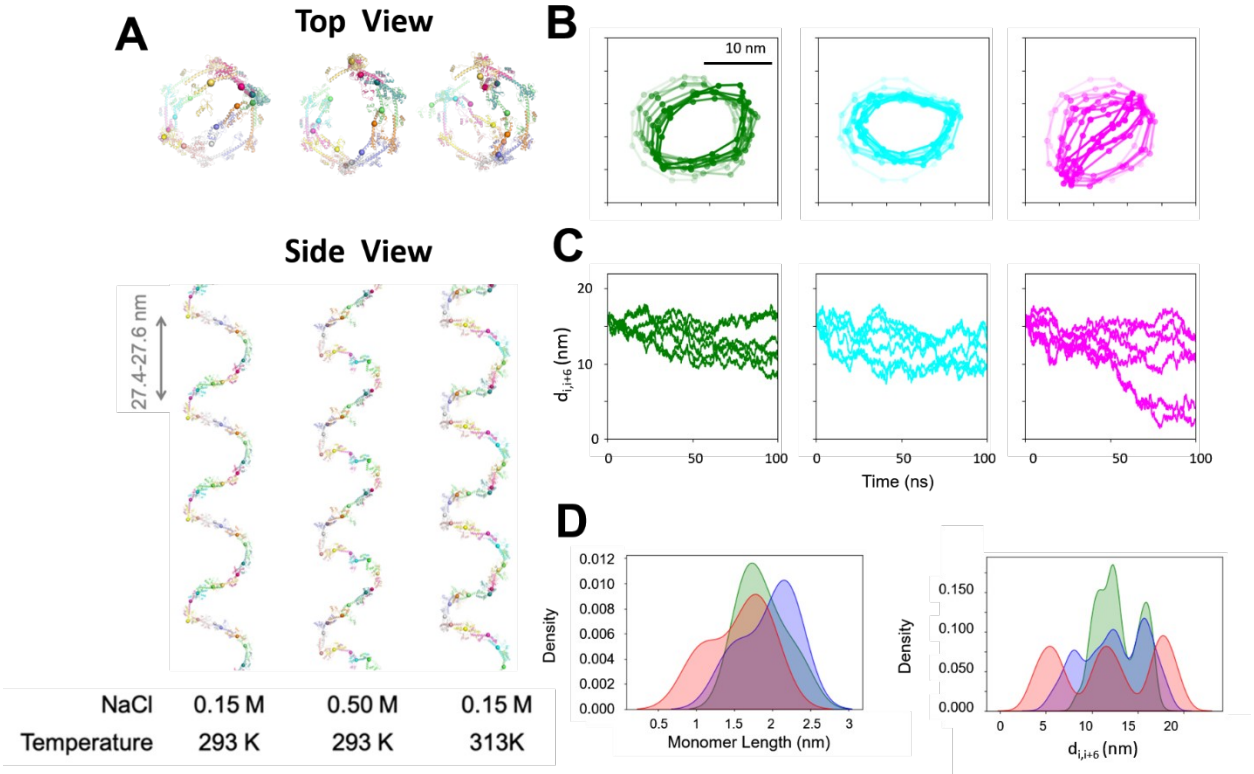

Figure 2. (A) Top and side views of our AA filament simulations taken from a final snapshot at 100 ns. The C_α atoms of residues 22 and 68 that were used as endpoints to define the monomer length are shown as spheres, color-coded per monomer (also see Figure S6). **(B)** Time evolution (100 ns, color-coded from light, 0 ns, to dark, 100 ns) of the filament circumference projected on the XY plane. Knots represent the centers of mass of a monomer. The colors correspond to the simulation conditions with green for standard (0.15 M NaCl, 293

K), cyan for high salt (0.50 M NaCl, 293 K) and magenta for high temperature (0.15 M NaCl, 313 K). The same color scheme is used in (C) and (D). **(C)** Time evolution of the distance between the heavy-atom center of the i^{th} and $(i+6)^{th}$ H-NS monomers $d_{i, i+6}$. As 12 monomers in each model were simulated, the six traces in each plot represent $d_{i, i+6}$ of the six pairs. **(D)** The distributions of monomer length and diameters at the end of the simulations.

During the simulations, thermal fluctuations led to deviations of the filament from the initial superhelix that obeyed strict crystallographic symmetry. Some monomers irregularly located along the filament contributed more than others to the filament deformation (Figure 2B-2C). This heterogeneity was apparent in the uneven distribution of monomer-monomer angles within the superhelix projections in the XY plane (Figure 2B) and of the superhelical half-turn distances, $d_{i, i+6}$, calculated as the distance between the heavy-atom center (using residues 2 to 82) of the i^{th} and $(i+6)^{th}$ H-NS monomers. Both phenomena were particularly pronounced at high temperature. To identify the basis of this heterogeneity in H-NS filament dynamics, we analyzed the distribution of the monomer length (defined as the Cα distance between residues 22 and 68 which bound the subset of H-NS that lay near the helix, see Figure S6) and the distribution of $d_{i, i+6}$. High salinity or temperature only slightly broadened the distribution of the monomer length, consistent with the subtle changes we observed for the helical pitch. However, the distribution of $d_{i, i+6}$ after 100 ns of simulation was markedly broadened at high temperature, showing a heterogeneous trimodal shape with equally populated peaks at 5, 12 and 18 nm. In comparison the distribution showed a much narrower landscape with peaks at 10, 12 and 16 nm for 0.15 M NaCl/293 K. The 500 mM NaCl condition showed intermediate breadth with peaks at 8, 13 and 16 nm (Figure 2D). These results suggest that the increase in temperature and, to a lesser extent in salinity, distort the H-NS filament. This distortion results from dynamic heterogeneities among the monomers, where strain is unevenly distributed along the helix.

To understand the mechanism underlying the monomer heterogeneity, the domains of each H-NS monomer were inspected. In our previous studies,[9, 10] we showed that site1 dimers are generally more stable than site2 dimers, and that specific salt bridges in the site2 dimers (such as K54–E74' and K57–D68', where the apostrophe denotes residues from the second chain) mediate heat or salt–induced melting of site2. In agreement, site2 also displayed a higher flexibility than site1 in our filament simulations at 0.15 M NaCl, 293 K (local Cα RMSD were 2.2 ± 0.1 Å and 1.8 ± 0.1 Å, respectively). Although the salt bridges K54-E74' and K57–D68' were present in the final snapshots at 100 ns simulation at high temperature or salinity, they formed and reformed throughout the simulation. Furthermore, the K54-E74' and K57–D68' salt bridges in the high temperature or salinity simulations showed more frequent breaking and forming when compared with the 0.15 M NaCl and 293 K simulations (Figure 3D). The transient loss of these salt bridges and the associated increase in the flexibility of the site2 backbone is likely a direct response of H-NS to environmental changes, causing the global deformation of the filament. Notably, our previous free-energy simulations suggested that the disassociation energy of the site2 dimer was lowered by more than 2 kcal/mol[10] at high salinity (0.50 M NaCl) or temperature (313 K). Since the dissociation of the entire H-NS filament has a strong thermodynamic driving force (*2xN* kcal/mol where *N* is the number of pairs in the filament), the monomer heterogeneity and filament deformation observed in our AA or CG simulations may only represent the initial response of the H-NS filament to environmental changes.

Our previous studies elucidated the molecular mechanism of H-NS autoinhibition:[10] Melting of site2 (e.g. due to high temperature) allows the DNAbd and site2–DNAbd linker to associate with site1 dimers, thereby resulting in a DNA-binding incompetent form. The conformational states of the DNAbd in the H-NS filament have not been investigated. In all our simulations, we observed that in absence of bound DNA, and with intact site2 dimers, the DNAbds were mostly residing in

proximity of the H-NS filament (~78% of DNAbds had a centroid distance below 4 nm), despite being flexibly attached to site2 by a ten-residue linker. Within a distance cutoff of 8 Å, most contacts between DNAbd and the site1–site2 fragment in the H-NS filament were polar or ionic. However, the interactions were transient and occurred with different binding modes. On the filament, contacts were contributed by residues located on the central part of helix3 that connects site1 and site2 (R41, E42, E43, E44, S45, A46 and A47). On the DNAbd, contacts were established by two stretches of residues (G104, E105, T106, K107, and G113, R114, P116, A117) that line one site of this domain (Figure 3B). It was previously shown that residues G113 to A117 are involved in DNA interactions where G113 and R114 form the QGR motif.[50] Thus, we speculate that the fuzzy self-association of the DNAbd with the filament backbone may mildly oppose DNA binding, and present a protection against non-specific DNA associations. The DNAbd–helix3 interactions in the filament are however structurally different from the self-associations that block DNA binding in the autoinhibited dimeric form of H-NS, because in the latter the association involves site1 and is driven by the basic site2–DNAbd linker, which is also a key element for DNA binding.[9, 10, 25] Increasing salinity and temperature affected the DNAbd–helix3 association differently compared to the standard condition (0.15 M NaCl and 293 K): DNAbd was more likely to contact helix3 at a higher temperature (313 K), but less likely to do so at a higher NaCl concentration (0.50 M). The effect of salinity is explained by providing a stronger screening effect that weakens the ionic and polar intramolecular contacts. The observation that temperature promotes the self-association may involve entropic effects favoring release of bound solvent ions.

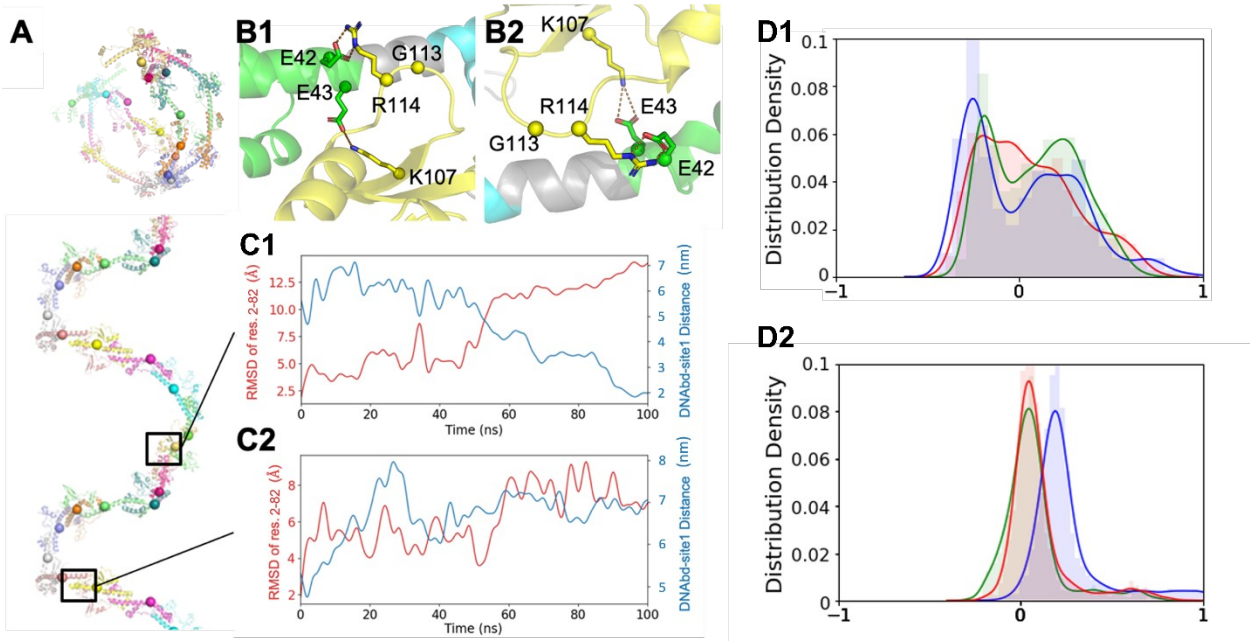

Figure 3. (A) Top and side views of the H-NS filament in the final snapshot of our MD simulation at high temperature (0.15 M NaCl, 313 K). **(B)** Examples of DNAbd–site1 interactions that alter the filament stability at 313 K. Electrostatic interactions between $K107^{DNAbd}$–$E43^{site1}$ and $R114^{DNAbd}$–$E42^{site1}$ were often observed. **(C)** Time evolutions of the monomeric backbone RMSD (residues 2-86, the red plot) and the corresponding DNAbd–site1 centroid distance (the blue plot). **(D)** Distribution of the sidechain N-O distances of R54 and E74' (D1), K57 and D68' (D2) during the last 20 ns at 0.15 M NaCl, 293 K (green), 0.50 M NaCl, 293 K (blue), and 0.15 M NaCl, 313 K (red). Baseline is the initial model.

Additional to potentially affecting DNA binding, we also found that the DNAbd backbinding reduced the stability of the H-NS filament in our simulations. We analyzed the correlation between the local backbone RMSD of each monomer and its DNAbd–helix3 centroid distance in all our filament simulations without bound DNA (Table S2). 46% of the monomers with DNAbd–helix3 contacts showed a strong anticorrelation between the RMSD and the DNAbd–helix3 centroid distance, which indicates that the association of DNAbd and the filament could increase the backbone RMSD and induce the monomer distortion. Moreover, 63% of monomers without DNAbd–helix3 contacts also lacked a correlation between the RMSD and the centroid distance, suggesting certain independence of these two domains (see examples in Figure 3C). In other words, the transient interactions between the filament and the DNAbds likely distorted the monomer backbone, and thus deviated the H-NS filament from a perfect superhelix. This effect could reduce filament stability, especially at a high temperature (Figure 3A). Conversely, in a DNA-bound state, the same effect may be diminished and enhance filament stability, a possibility explored in the following.

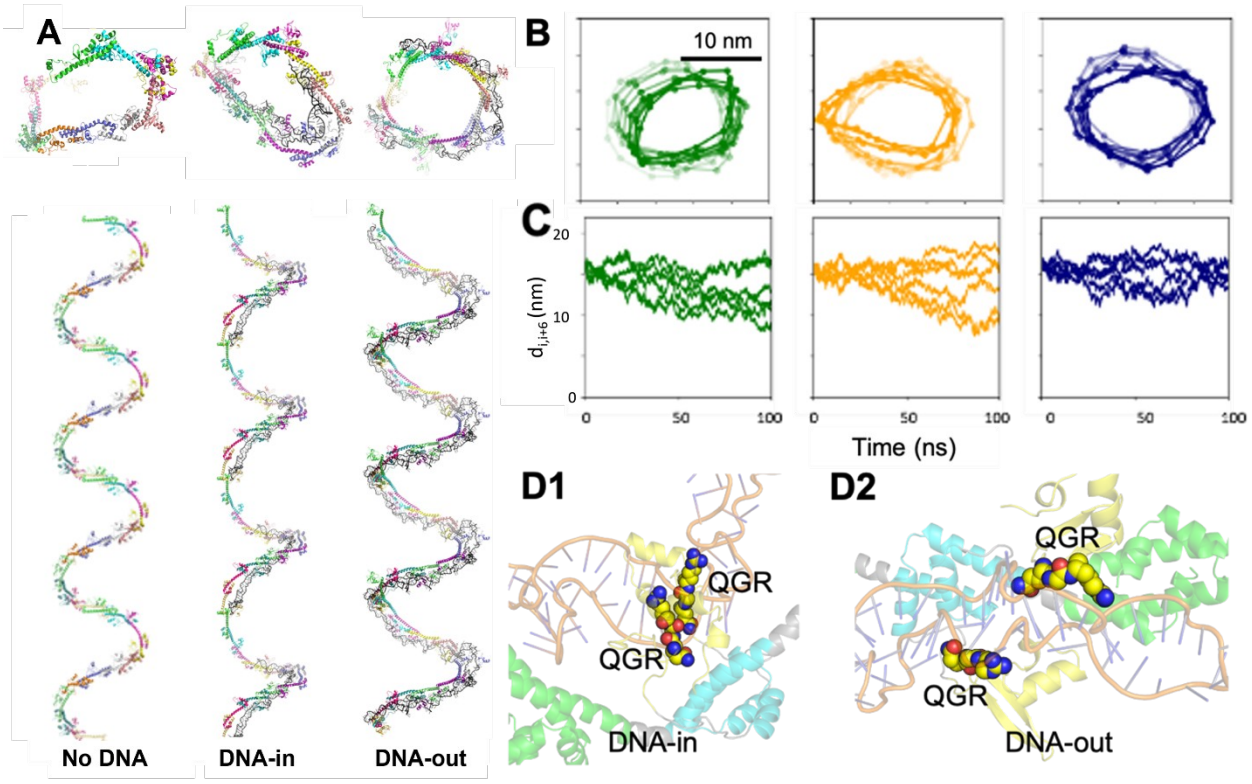

Figure 4. (A) Top and side views of our DNA-free and DNA-bound simulations (0.15 M NaCl, 293 K). H-NS is in rainbow color mode and DNA is black. Specific illustration of the models of H-NS–DNA complex is shown in Figure S7. **(B)** Time evolution (from light to dark) of the filament circumference projected onto the XY plane. Knots represent the centers of mass of a monomer **(C)** Time evolution of the distance between the heavy-atom center of the i^{th} and $(i+6)^{th}$ H-NS monomers. **(D)** Cartoon illustration of DNAbd interactions with DNA in two different models.

One widely accepted DNA-binding mode of H-NS is that H-NS can spread along DNA and stiffen the DNA molecule. In order to gain molecular insight, we built two DNA-bound H-NS filament models (Figure S7) with DNA bound to the interior of the superhelix (DNA-in) or to the exterior of the superhelix (DNA-out). After 100 ns of simulation at 293K and 0.15 M NaCl, the DNAbd remained in close contacts with the DNA duplex in all the DNA-bound simulations,

indicating the high stability of the complexes. Further, the QGR motif, with the sidechains of Q112 and R114 extended to maximize the contacts with DNA (Figure 4D), contributed significantly to the stable binding. We also observed other less specific interactions between DNAbd and DNA, involving residues like R93, K96, K120, and K121. Clearly these positively charged residues allowed generally binding to negatively charged DNA molecules. In addition, our observation supports the binding modes by QGR and R93,[16] and supported that the interface of DNA and H-NS also extends to the site2–DNAbd linker.[25]

DNA binding generally reduced the flexibility of the entire H-NS filament, and this effect was more pronounced in the DNA-out simulations than in the DNA-in simulations. This effect is supported by an estimation of the persistence length, *L*, from the H-NS filament simulations (Figure 5). Without DNA binding, L was reduced by increased salinity or temperature, consistent with our observations. With DNA binding, there was an increase in *L* of 9% and 130% for the DNA-in and DNA-out models respectively. Our estimates of *L* correlate with prior salt dependent force-based measurements of DNA elasticity.[51] In those measurements, *L* of the DNA increased from 50 to 130 nm with an increasing H-NS concentration. Furthermore, increased salinity resulted in a lower *L*, which we also saw in the simulations (Figure 5). In addition to changes in *L*, the H-NS superhelical structure was well preserved in the simulations of the DNA-out model, whereas the filament distortion was only slightly reduced in the DNA-in simulations compared with the DNA-free simulations (Figure 4B-4C). Thus, the H-NS filament–DNA complex was stiffer than the DNA molecule (with a *L* of ~50 nm) or the filament alone, thereby supporting the above-mentioned stiffening model. Comparing the DNA-in and DNA-out models and their simulations, we found that the DNA-in model allowed 20 times more contacts between the DNA strands and the site1, which could cause bending of the polymerization domain (Figure 4D1) as well as disruption of base pairing in DNA. Notably, we modeled an extreme case that all DNAbds of the H-NS filament were bound to the DNA molecule on one side of the filament. If only some of the DNAbds were bound to DNA in the same way, there would be less distortion in the DNA-in model. The other DNAbds might engage in binding to another DNA molecule, thereby producing a bridging DNA-binding mode.

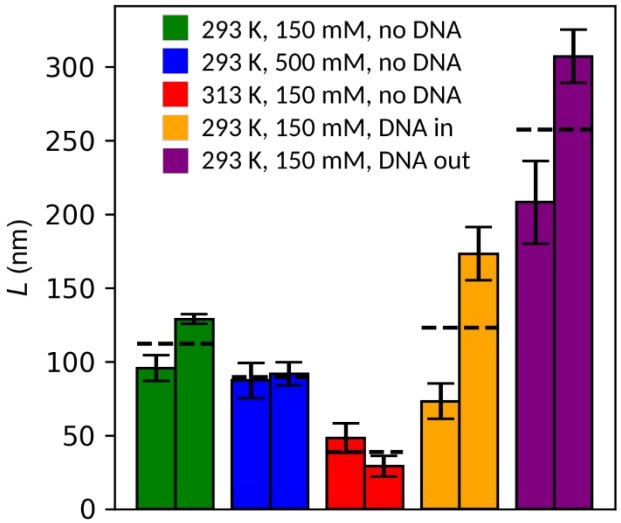

Figure 5. Persistence length of the H-NS filaments estimated from the all-atom MD simulations. Replica simulations are shown for each temperature, NaCl concentration, and DNA-bound state of the system. Error bars from the linear fits described in the SM are shown along with the average of the two replicas as dashed lines.

With or without DNA, H-NS filaments constitute a complex dynamical system that could experimentally only be studied using low-resolution methods.[8-10, 14, 15, 40, 51, 52] Herein, we have used all-atom and coarse-grained modeling to investigate H-NS filaments. Our simulations recapitulated the experimental observations that the stability of H-NS polymers weakens as temperature and salinity increase, and that this destabilization is mediated by salt bridges in site2 dimers. Herein, the effect of salt less pronounced than the effect of temperature, in line with previous experimental observations.[8-10] Additionally, our large-scale simulation provided atomistic insights into H-NS filament dynamics underlying its environment sensing function. We observed that the temperature- and salt-induced destabilization of the filament correlates with a marked conformational heterogeneity of the monomers in the filament. Monomer heterogeneity has already been shown as a dynamic feature related to functions in the other biological filaments like actin.[53] Our observations of such a feature in the H-NS filament, which is structurally distinct from the actin filament, suggests that this is a more general feature among biological filaments. We also observed a tendency of the DNAbd to loosely associate with the helix3 region that links site1 and site2 dimers in the filament. This backbinding led to strains that tended to deform the filament. Being based on mostly polar interactions, backbinding, and hence filament straining, was enhanced by high temperature, but decreased by salinity. Hence, the backbinding of the DNAbd might contribute to temperature-induced filament destabilization in the absence of DNA while conversely lead to stabilization in the presence of DNA. The fuzzy interactions with the filament involved the DNA-binding regions of the DNAbd, raising the possibility that this self-association is mildly opposing DNA binding, possibly to reduce non-specific binding. Finally, we explored two models for H-NS polymerization along a DNA filament. In agreement with experimental observations, we noted that the H-NS–DNA complex had an increased stability compared to apo-H-NS filaments. Our investigations also revealed greater stability of the ‘DNA-out’ model, where the DNA strand runs on the outside of the H-NS filament superhelix, as compared to the ‘DNA-in’ model. Considering the enhanced stability is more attuned with the function and mechanism of H-NS for DNA association, the ‘DNA-out’ model may of greater biological significance. Collectively, our study provides unprecedented molecular insight into the dynamics, architecture, and environmental sensing ability of the filament stage of H-NS in presence and absence of DNA.

Acknowledgments
We thank Dr Chenyi Liao (Dalian Institute of Chemical Physics) for helpful discussion and the Vermont Advanced Computing Core for supercomputing resources. X.Z. and J.L. was partially supported by an NSF award (CHE-1945394 to J. L.); J.M.R. was supported by an NIH award (R01GM129431 to J.L.); S.T.S. was supported by the U.S. Army Research Office (Grant 71015-CH-YIP). Research by S.T.A was supported by the King Abdullah University of Science and Technology (KAUST).

Supporting Information Available
Computational methods are available in the SI. In addition, various distributions of RMSD and centroid distances for the superhelical models (S1-4), an illustration of the CG filament model (S5), the definition of the monomer length (S6), and the H-NS–DNA complexes (S7) are all provided. Two movies showing the simulated H-NS filaments in control verses high temperature (Movie 1) and control verses high salt (Movie 2) are also included.

References:

1. Dillon, S. C.; Dorman, C. J., Bacterial nucleoid-associated proteins, nucleoid structure and gene expression. *Nature Reviews Microbiology* **2010,** *8* (3), 185-195.

2. Hudson, W. H.; Ortlund, E. A., The structure, function and evolution of proteins that bind DNA and RNA. *Nature reviews Molecular cell biology* **2014,** *15* (11), 749-760.

3. Dame, R. T.; Rashid, F.-Z. M.; Grainger, D. C., Chromosome organization in bacteria: mechanistic insights into genome structure and function. *Nature Reviews Genetics* **2020,** *21* (4), 227-242.

4. Azam, T. A.; Ishihama, A., Twelve species of the nucleoid-associated protein from Escherichia coli: sequence recognition specificity and DNA binding affinity. *Journal of Biological Chemistry* **1999,** *274* (46), 33105-33113.

5. Tendeng, C.; Bertin, P. N., H-NS in Gram-negative bacteria: a family of multifaceted proteins. *Trends Microbiol.* **2003,** *11* (11), 511-518.

6. Dorman, C. J., H-NS: a universal regulator for a dynamic genome. *Nat. Rev. Microbiol.* **2004,** *2* (5), 391-400.

7. Grainger, D. C., Structure and function of bacterial H-NS protein. *Biochem. Soc. Trans.* **2016,** *44*, 1561-1569.

8. Arold, S. T.; Leonard, P. G.; Parkinson, G. N.; Ladbury, J. E., H-NS forms a superhelical protein scaffold for DNA condensation. *Proc. Natl. Acad. Sci. U. S. A.* **2010,** *107* (36), 15728-15732.

9. Shahul Hameed, U. F.; Liao, C.; Radhakrishnan, A. K.; Huser, F.; Aljedani, S. S.; Zhao, X.; Momin, A. A.; Melo, F. A.; Guo, X.; Brooks, C., H-NS uses an autoinhibitory conformational switch for environment-controlled gene silencing. *Nucleic acids research* **2019,** *47* (5), 2666-2680.

10. Zhao, X.; Hameed, U. F. S.; Kharchenko, V.; Liao, C.; Huser, F.; Remington, J. M.; Radhakrishnan, A. K.; Jaremko, M.; Jaremko, Ł.; Arold, S. T., Molecular basis for the adaptive evolution of environment-sensing by H-NS proteins. *Elife* **2021,** *10*, e57467.

11. Lateana, A.; Brandi, A.; Falconi, M.; Spurio, R.; Pon, C. L.; Gualerzi, C. O., Identification of a Cold Shock Transcriptional Enhancer of the Escherichia-Coli Gene Encoding Nucleoid Protein H-NS. *Proc. Natl. Acad. Sci. U. S. A.* **1991,** *88* (23), 10907-10911.

12. Spurio, R.; Falconi, M.; Brandi, A.; Pon, C. L.; Gualerzi, C. O., The oligomeric, structure of nucleoid protein H-NS is necessary for recognition of intrinsically curved DNA and for DNA bending. *EMBO J.* **1997,** *16* (7), 1795-1805.

13. Stella, S.; Falconi, M.; Lammi, M.; Gualerzi, C. O.; Pon, C. L., Environmental control of the in vivo oligomerization of nucleoid protein H-NS. *J. Mol. Biol.* **2006,** *355* (2), 169-174.

14. Dame, R. T.; Wyman, C.; Goosen, N., H-NS mediated compaction of DNA visualised by atomic force microscopy. *Nucleic Acids Res.* **2000,** *28* (18), 3504-3510.

15. Dame, R. T.; Wyman, C.; Goosen, N., Structural basis for preferential binding of H-NS to curved DNA. *Biochimie* **2001,** *83* (2), 231-234.

16. Bloch, V.; Yang, Y. S.; Margeat, E.; Chavanieu, A.; Auge, M. T.; Robert, B.; Arold, S.; Rimsky, S.; Kochoyan, M., The H-NS dimerization domain defines a new fold contributing to DNA recognition. *Nat. Struct. Biol.* **2003,** *10* (3), 212-218.

17. Dame, R. T.; Luijsterburg, M. S.; Krin, E.; Bertin, P. N.; Wagner, R.; Wuite, G. J. L., DNA bridging: a property shared among H-NS-like proteins. *J. Bacteriol.* **2005,** *187* (5), 1845-1848.

18. Dame, R. T.; Noom, M. C.; Wuite, G. J. L., Bacterial chromatin organization by H-NS protein unravelled using dual DNA manipulation. *Nature* **2006,** *444* (7117), 387-390.

19. Vreede, J.; Dame, R. T., Predicting the effect of ions on the conformation of the H-NS dimerization domain. *Biophys. J.* **2012,** *103* (1), 89-98.

20. van der Valk, R. A.; Vreede, J.; Qin, L.; Moolenaar, G. F.; Hofmann, A.; Goosen, N.; Dame, R. T., Mechanism of environmentally driven conformational changes that modulate H-NS DNA-bridging activity. *Elife* **2017,** *6*.

21. Riccardi, E.; van Mastbergen, E. C.; Navarre, W. W.; Vreede, J., Predicting the mechanism and rate of H-NS binding to AT-rich DNA. *PLoS Comp. Biol.* **2019,** *15* (3).

22. Qin, L.; Bdira, F. B.; Sterckx, Y. G. J.; Volkov, A. N.; Vreede, J.; Giachin, G.; van Schaik, P.; Ubbink, M.; Dame, Remus T., Structural basis for osmotic regulation of the DNA binding properties of H-NS proteins. *Nucleic Acids Res.* **2020,** *48* (4), 2156-2172.

23. Fang, F. C.; Rimsky, S., New insights into transcriptional regulation by H-NS. *Curr. Opin. Microbiol.* **2008,** *11* (2), 113-120.

24. Liu, Y. J.; Chen, H.; Kenney, L. J.; Yan, J., A divalent switch drives H-NS/DNA-binding conformations between stiffening and bridging modes. *Genes Dev.* **2010,** *24* (4), 339-344.

25. Gao, Y.; Foo, Y. H.; Winardhi, R. S.; Tang, Q.; Yan, J.; Kenney, L. J., Charged residues in the H-NS linker drive DNA binding and gene silencing in single cells. *Proceedings of the National Academy of Sciences* **2017,** *114* (47), 12560-12565.

26. Shindo, H.; Iwaki, T.; Ieda, R.; Kurumizaka, H.; Ueguchi, C.; Mizuno, T.; Morikawa, S.; Nakamura, H.; Kuboniwa, H., Solution Structure of the DNA-Binding Domain of a Nucleoid-Associated Protein, H-Ns, from Escherichia-Coli. *FEBS Lett.* **1995,** *360* (2), 125-131.

27. Ceschini, S.; Lupidi, G.; Coletta, M.; Pon, C. L.; Fioretti, E.; Angeletti, M., Multimeric self-assembly equilibria involving the histone-like protein H-NS - A thermodynamic study. *J. Biol. Chem.* **2000,** *275* (2), 729-734.

28. Smyth, C. P.; Lundback, T.; Renzoni, D.; Siligardi, G.; Beavil, R.; Layton, M.; Sidebotham, J. W.; Hinton, J. C. D.; Driscoll, P. C.; Higgins, C. F.; Ladbury, J. E., Oligomerization of the chromatin-structuring protein H-NS. *Mol. Microbiol.* **2000,** *36* (4), 962-972.

29. Renzoni, D.; Esposito, D.; Pfuhl, M.; Hinton, J. C. D.; Higgins, C. F.; Driscoll, P. C.; Ladbury, J. E., Structural characterization of the N-terminal oligomerization domain of the bacterial chromatin-structuring protein, H-NS. *J. Mol. Biol.* **2001,** *306* (5), 1127-1137.

30. Schroder, O.; Tippner, D.; Wagner, R., Toward the three-dimensional structure of the Escherichia coli DNA-binding protein H-NS: A CD and fluorescence study. *Biochemical and Biophysical Research Communications* **2001,** *282* (1), 219-227.

31. Esposito, D.; Petrovic, A.; Harris, R.; Ono, S.; Eccleston, J. F.; Mbabaali, A.; Haq, I.; Higgins, C. F.; Hinton, J. C. D.; Driscoll, P. C.; Ladbury, J. E., H-NS oligomerization domain structure reveals the mechanism for high order self-association of the intact protein. *J. Mol. Biol.* **2002,** *324* (4), 841-850.

32. Nye, M. B.; Taylor, R. K., Vibrio cholerae H-NS domain structure and function with respect to transcriptional repression of ToxR regulon genes reveals differences among H-NS family members. *Mol. Microbiol.* **2003,** *50* (2), 427-444.

33. Yamanaka, Y.; Winardhi, R. S.; Yamauchi, E.; Nishiyama, S.-i.; Sowa, Y.; Yan, J.; Kawagishi, I.; Ishihama, A.; Yamamoto, K., Dimerization site 2 of the bacterial DNA-binding protein H-NS is required for gene silencing and stiffened nucleoprotein filament formation. *J. Biol. Chem.* **2018,** *293* (24), 9496-9505.

34. Hinton, J. C. D.; Santos, D. S.; Seirafi, A.; Hulton, C. S. J.; Pavitt, G. D.; Higgins, C. F., EXPRESSION AND MUTATIONAL ANALYSIS OF THE NUCLEOID-ASSOCIATED PROTEIN H-NS OF SALMONELLA-TYPHIMURIUM. *Mol. Microbiol.* **1992,** *6* (16), 2327-2337.

35. Japaridze, A.; Renevey, S.; Sobetzko, P.; Stoliar, L.; Nasser, W.; Dietler, G.; Muskhelishvili, G., Spatial organization of DNA sequences directs the assembly of bacterial chromatin by a nucleoid-associated protein. *J. Biol. Chem.* **2017,** *292* (18), 7607-7618.

36. Badaut, C.; Williams, R.; Arluison, V.; Bouffartigues, E.; Robert, B.; Buc, H.; Rimsky, S., The degree of oligomerization of the H-NS nucleoid structuring protein is related to specific binding to DNA. *J. Biol. Chem.* **2002,** *277* (44), 41657-41666.

37. Cordeiro, T. N.; Schmidt, H.; Madrid, C.; Juárez, A.; Bernadó, P.; Griesinger, C.; García, J.; Pons, M., Indirect DNA Readout by an H-NS Related Protein: Structure of the DNA Complex of the C-Terminal Domain of Ler. *PLoS Pathog* **2011,** *7* (11), e1002380.

38. Gordon, B. R. G.; Li, Y. F.; Cote, A.; Weirauch, M. T.; Ding, P. F.; Hughes, T. R.; Navarre, W. W.; Xia, B.; Liu, J., Structural basis for recognition of AT-rich DNA by unrelated xenogeneic silencing proteins. *Proc. Natl. Acad. Sci. U. S. A.* **2011,** *108* (26), 10690-10695.

39. Rosselli-Murai, L. K.; Sforca, M. L.; Sassonia, R. C.; Azzoni, A. R.; Murai, M. J.; de Souza, A. P.; Zeri, A. C., Structural characterization of the H-NS protein from Xylella fastidiosa and its interaction with DNA. *Arch. Biochem. Biophys.* **2012,** *526* (1), 22-28.

40. Liang, Y.; van der Valk, R. A.; Dame, R. T.; Roos, W. H.; Wuite, G. J. L., Probing the mechanical stability of bridged DNA-H-NS protein complexes by single-molecule AFM pulling. *Sci. Rep.* **2017,** *7*.

41. Gordon, B. R.; Li, Y.; Cote, A.; Weirauch, M. T.; Ding, P.; Hughes, T. R.; Navarre, W. W.; Xia, B.; Liu, J., Structural basis for recognition of AT-rich DNA by unrelated xenogeneic silencing proteins. *Proceedings of the National Academy of Sciences* **2011,** *108* (26), 10690-10695.

42. Arold, S. T.; Leonard, P. G.; Parkinson, G. N.; Ladbury, J. E., H-NS forms a superhelical protein scaffold for DNA condensation. *Proceedings of the National Academy of Sciences* **2010,** *107* (36), 15728-15732.

43. Riccardi, E.; Van Mastbergen, E. C.; Navarre, W. W.; Vreede, J., Predicting the mechanism and rate of H-NS binding to AT-rich DNA. *PLoS computational biology* **2019,** *15* (3), e1006845.

44. Qin, L.; Bdira, F. B.; Sterckx, Y. G.; Volkov, A. N.; Vreede, J.; Giachin, G.; van Schaik, P.; Ubbink, M.; Dame, R. T., Structural basis for osmotic regulation of the DNA binding properties of H-NS proteins. *Nucleic acids research* **2020,** *48* (4), 2156-2172.

45. Dersch, P.; Schmidt, K.; Bremer, E., SYNTHESIS OF THE ESCHERICHIA-COLI K-12 NUCLEOID-ASSOCIATED DNA-BINDING PROTEIN H-NS IS SUBJECTED TO GROWTH-PHASE CONTROL AND AUTOREGULATION. *Mol. Microbiol.* **1993,** *8* (5), 875-889.

46. Rafiei, N.; Cordova, M.; Navarre, W. W.; Milstein, J. N., Growth Phase-Dependent Chromosome Condensation and Heat-Stable Nucleoid-Structuring Protein Redistribution in Escherichia coli under Osmotic Stress. *J. Bacteriol.* **2019,** *201* (23).

47. Dersch, P.; Susanne, K.; Erhard, B., The nucleoid-associated DNA-bindingprotein H-NS is required for the efficient adaptation of Escherichia coil K-12 to a cold environment. *Mol Gen Genet* **1994,** *245*, 255-259.

48. Ali, S. S.; Soo, J.; Rao, C.; Leung, A. S.; Ngai, D. H.-M.; Ensminger, A. W.; Navarre, W. W., Silencing by H-NS Potentiated the Evolution of Salmonella. *PLoS Path.* **2014,** *10* (11).

49. Nishino, K.; Yamaguchi, A., Role of histone-like protein H-NS in multidrug resistance of Escherichia coli. *J. Bacteriol.* **2004,** *186* (5), 1423-1429.

50. Ueguchi, C.; Suzuki, T.; Yoshida, T.; Tanaka, K.; Mizuno, T., Systematic mutational analysis revealing the functional domain organization of Escherichia coli nucleoid protein H-NS. *J. Mol. Biol.* **1996,** *263* (2), 149-162.

51. Amit, R.; Oppenheim, A. B.; Stavans, J., Increased bending rigidity of single DNA molecules by H-NS, a temperature and osmolarity sensor. *Biophys. J.* **2003,** *84* (4), 2467-2473.

52. Winardhi, R. S.; Castang, S.; Dove, S. L.; Yan, J., Single-Molecule Study on Histone-Like Nucleoid-Structuring Protein (H-NS) Paralogue in Pseudomonas aeruginosa: MvaU Bears DNA Organization Mode Similarities to MvaT. *PLoS One* **2014,** *9* (11).

53. Fan, J.; Saunders, M. G.; Voth, G. A., Coarse-graining provides insights on the essential nature of heterogeneity in actin filaments. *Biophysical journal* **2012,** *103* (6), 1334-1342.